Cell Counting Kit-8

Cell Proliferation Assay and Cytotoxicity Assay

Technical Manual

for 100 tests, 500 tests, 1000 tests, 3000 tests, and 10000 tests

General Information

Cell Counting Kit-8 (CCK-8) allows very convenient assays by utilizing Dojindo's highly water-soluble tetrazolium salt. WST-8 [2-(2-methoxy-4-nitrophenyl)-3-(4-nitrophenyl)-5-(2,4-disulfophenyl)-2*H*-tetrazolium, monosodium salt] produces a water-soluble formazan dye upon reduction in the presence of an electron mediator, as shown in Figure 1.

CCK-8 is a one-bottle solution; no premixing of components is required. CCK-8, being nonradioactive, allows sensitive colorimetric assays for the determination of the number of viable cells in cell proliferation and cytotoxicity assays. WST-8 is reduced by dehydrogenases in cells to give an orange colored product (formazan), which is soluble in the tissue culture medium (Figure 2). The amount of the formazan dye generated by dehydrogenases in cells is directly proportional to the number of living cells.

Figure 3 shows that the cell proliferation assay using CCK-8 correlates well with the [^{3}H]-thymidine incorporation assay. Thus, the CCK-8 assay can also be substituted for the [^{3}H]-thymidine incorporation assay. As shown in Figure 4, the detection sensitivity using CCK-8 is higher than assays using other tetrazolium salts such as MTT, XTT, MTS or WST-1.

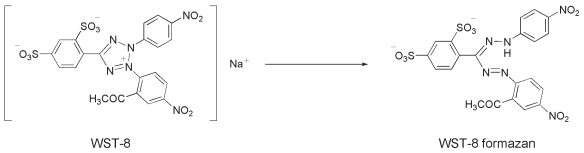

Figure 1. Structures of WST-8 and WST-8 formazan

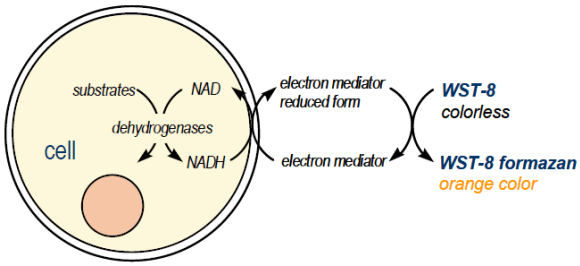

Figure 2. Principle of the cell viability detection with Cell Counting Kit-8

Kit Contents

- 100 tests :	1 ml	x	1
- 500 tests :	5 ml	x	1
- 1000 tests :	5 ml	x	2
- 3000 tests :	5 ml	x	6
- 10000 tests :	100 ml	x	1

Storage

Store at 0-5°C

CCK-8 is stable over one year at 0-5°C with protection from light. Store it at -20°C for longer storage. Repeated thawing and freezing causes an increase in the background, which interferes with the assay. Please store the kit at 0-5°C for frequent use.

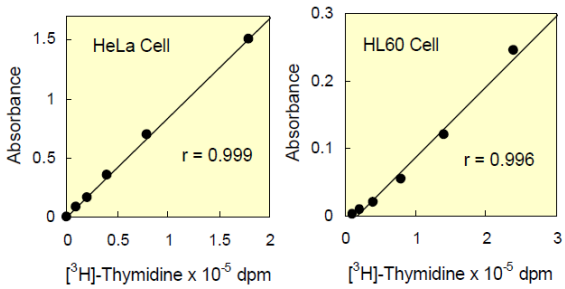

Figure 3 Correlation between CCK-8 assay and [^{3}H]-thymidine incorporation assay.

Medium : HeLa.....MEM, 10% FBS
HL60.....RPMI1640, 10% FBS
Reagent : [^{3}H]-Thymidine.....37 KBq/well
CCK-8.....10 µl/well
Incubation : [^{3}H]-Thymidine assay..... 4 hours
CCK-8.....3 hours

Required Equipment and Materials

- plate reader (450 nm filter)
- 96-well plate
- CO_2 incubator
- 10 µl and 100 - 200 µl multi-channel pipettes

General Protocol

Cell Number Determination

1. Inoculate cell suspension (100 µl/well) in a 96-well plate. Pre-incubate the plate in a humidified incubator (e.g., at 37 °C, 5% CO_2).
2. Add 10 µl of the CCK-8 solution to each well of the plate. *Be careful not to introduce bubbles to the wells, since they interfere with the O.D. reading.*
3. Incubate the plate for 1 - 4 hours in the incubator.
4. Measure the absorbance at 450 nm using a microplate reader.
   To measure the absorbance later, add 10 µl of 1% w/v SDS or 0.1 M HCl to each well, cover the plate and store it with protection from light at room temperature. No absorbance change should be observed for 24 hours.

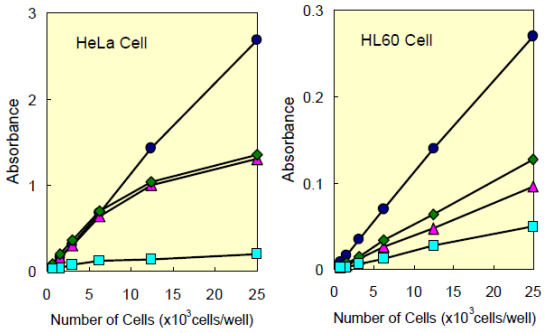

Figure 4 Cell number determination using CCK-8 and other reagents.

Medium : HeLa.....MEM, 10% FBS
HL60.....RPMI1640, 10% FBS
Incubation : HeLa.....37°C, 5 % CO_2, 2 hours
HL60.....37°C, 5 % CO_2, 3 hours
Detection : CCK-8 (●) ... 450 nm, XTT (◆)....450 nm
MTS (▲).....490 nm, MTT (■)....570 nm

Cell Proliferation and Cytotoxicity Assay

1. Dispense 100 µl of cell suspension (5000 cells/well) in a 96-well plate. Pre-incubate the plate for 24 hours in a humidified incubator (e.g., at 37°C, 5% CO_2).
2. Add 10 µl of various concentrations of substances to be tested to the plate.
3. Incubate the plate for an appropriate length of time (e.g., 6, 12, 24 or 48 hours) in the incubator.
4. Add 10 µl of CCK-8 solution to each well of the plate.
   Be careful not to introduce bubbles to the wells, since they interfere with the O.D. reading.
5. Incubate the plate for 1 - 4 hours in the incubator.
6. Measure the absorbance at 450 nm using a microplate reader.
   To measure the absorbance later, add 10 µl of 1% w/v SDS or 0.1 M HCl to each well, cover the plate and store it with protection from light at room temperature. No absorbance change should be observed for 24 hours.

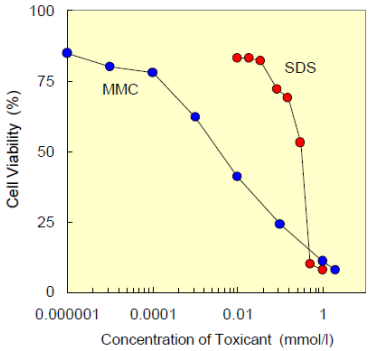

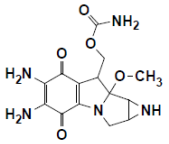

mitomycin-C (MMC)

$CH_3(CH_2)_{11}$-OSO_3Na

Dodecylsulfate, sodium salt (SDS)

Figure 5. Toxicological test of chemicals using CCK-8.

Cell line : HeLa
Culture medium : MEM, 10% FBS
Chemicals : Mitomycin-C (MMC),
Dodecylsulfate, sodium salt (SDS)
Incubation : 37°C, 5% CO_2, 2 hours
Detection : 450 nm, Reference : 650 nm

Precautions

1. Since the CCK-8 assay is based on the dehydrogenase activity detection in viable cells, conditions or chemicals that affect dehydrogenase activity in viable cells may cause discrepancy between the actual viable cell number and the cell number determined using the CCK-8 assay.
2. WST-8 may react with reducing agents to generate WST-8 formazan. Please check the background O.D. if reducing agents are used in cytotoxicity assays or cell proliferation assays.
3. Be careful not to introduce bubbles to the wells, since they interfere with the O.D. reading.
4. If the sterilization of the CCK-8 solution is necessary, please filter the solution with a 0.2 µm membrane.
5. The incubation time varies by the type and number of cells in a well. Generally, leukocytes give weak coloration, thus a long incubation time (up to 4 hours) or a large number of cells (~10^5 cells/well) may be necessary.
6. Measure and subtract the O.D. at 600 nm or higher from that of sample if there is a high turbidity in the cell suspension.

Frequently Asked Questions

1. How many cells should there be in a well?
For adhesive cells, at least 1000 cells are necessary per well (100 µl medium). For leukocytes, at least 2500 cells are necessary per well (100 µl medium) because of low sensitivity. The recommended maximum number of cells per well for the 96-well plate is 25000. If a 24-well or 6-well plate is used for this assay, please calculate the number of cells per well accordingly, and adjust the volume of the CCK-8 solution in a well to 10% of the total volume.

2. Does CCK-8 stain viable cells?
No. Since WST-8 and its formazan dye are highly water-soluble, CCK-8 cannot be utilized for cell staining purpose.

3. Does phenol red affect the assay?
No. The absorption value of phenol red in a culture medium can be removed by subtracting the absorption value of a blank solution from the absorption value of each well. Therefore, a medium containing phenol red is usable for the CCK-8 assay.

4. Is CCK-8 toxic to cells?
Since the toxicity of CCK-8 is so low, the same cells can be used for other cell proliferation assays such as the crystal violet assay, neutral red assay or DNA fluorometric assay after the CCK-8 assay is completed.

5. I do not have a 450 nm filter. What other filters can I use?
You can use filters with the absorbance between 430 and 490 nm, even though 450 nm filter gives the best sensitivity.

References

1. M. Ishiyama, Y. Miyazono, K. Sasamoto, Y. Ohkura and K. Ueno, *Talanta*, **1997**, *44*, 1299.
2. H. Tominaga, M. Ishiyama, F. Ohseto, K. Sasamoto, T. Hamamoto, K. Suzuki and M. Watanabe, *Anal. Commun.*, **1999**, *36*, 47.

If you need more information, please contact Dojindo technical service.

Dojindo Laboratories
2025-5 Tabaru, Mashiki-machi, Kamimashiki-gun, Kumamoto
861-2202, Japan Phone: +81-96-286-1515 Fax: +81-96-286-1525
E-mail: info@dojindo.co.jp Web: www.dojindo.co.jp

Dojindo Molecular Technologies,Inc.
Tel: +1-301-987-2667 Web:http://www.dojindo.com/
Dojindo EU GmbH
Tel: +49-89-3540-4805 Web: http://www.dojindo.eu.com/
Dojindo China Co., Ltd
Tel: +86-21-6427-2302 Web:http://www.dojindo.cn/

Cell Counting Kit-8 (CCK-8)　细胞增殖-毒性检测试剂盒

(100孔, 500孔, 1,000孔, 3,000孔以及10,000孔的规格)

注意事项:

1 第一次做实验时，建议先做几个孔摸索接种细胞的数量和加入CCK- 8试剂后的培养时间。

2 接种时注意细胞悬液一定要混匀，以避免细胞沉淀下来，导致每孔中的细胞数量不等，可以每接种几个孔就混匀一下。培养板周围一圈孔培养基容易挥发，为了减少误差，建议培养板的四边每孔只加培养基，而不作为指标检测孔。

3 培养时间根据细胞种类的不同和每孔内细胞数量的多少而异。一般情况下，白细胞较难显色，因此需要较长的CCK- 8反应时间或增加细胞数量 (～10^5个细胞/孔)。悬浮细胞与贴壁细胞相比较难显色。对于悬浮细胞，在加入CCK- 8培养1- 4小时后，可先从培养箱中取出，目测染色程度或用酶标仪测定决定。若显色困难，可将培养板放回培养箱，继续培养数小时后再确定。对于贴壁细胞，CCK- 8的培养时间一般为1- 4小时，但在培养30分钟左右即可取出肉眼观察显色程度 (根据细胞种类而定，需要摸索一下条件)。**注意：CCK- 8的最佳反应时间以具体显色的最佳时间为准。**

4 有条件的情况下建议采用多通道移液器，可以减少平行孔间的差异。加 CCK- 8试剂时，建议斜贴着培养板壁加，不要插到培养基液面下加，容易产生气泡，会干扰O.D值读数。

5 加 CCK- 8试剂时速度要快，减少试剂在移液器上的残留。为使CCK- 8试剂和培养基充分混匀，建议在加入CCK- 8试剂后轻轻振摇培养板。为了避免加样时由于CCK- 8试剂在枪头上的残留所带来的误差，可以在加样前用培养基稀释CCK- 8试剂并混匀后加样。

6 CCK- 8试剂中的WST®- 8会与还原剂反应生成WST® - 8甲臜，如果实验中有还原剂，请检查背景的O.D值，即在不含细胞的培养基中加入药物，然后加入CCK- 8试剂在一定时间内检测，和不加药物的培养基进行比较 (只加CCK- 8试剂)，如果O.D值明显偏高，则说明有反应。

7 若细胞培养时间较长，培养基颜色发生变化或pH发生变化，建议更换新鲜的培养基后再加CCK- 8试剂。含有酚红的培养基不影响本试剂盒做细胞活性的测定。

8 如果样品为高浑浊度的细胞悬液，建议设定600 nm (或600 nm以上) 作为参比波长，扣除参比波长的O.D值即可。

9 CCK- 8试剂对细胞的毒性非常低。它和活细胞内的脱氢酶持续反应使溶液颜色不断加深，O.D值不断增加 (注：活细胞内的脱氢酶是持续产生的) 。另外，其他的实验，例如中性红法或结晶紫法 ，也可在CCK- 8法检测完后继续进行。

10 如果要测定细胞的具体数量，建议先做一个标准曲线 (具体方法参见P3的 “ 制作标准曲线 ”)。

试剂内含

- 100 孔:	1 ml x 1 管
- 500 孔:	5 ml x 1 瓶
- 1,000 孔:	5 ml x 2 瓶
- 3,000 孔:	5 ml x 6 瓶
- 10,000 孔:	100 ml x 1 瓶

贮藏条件

CCK- 8在避光0- 5°C的条件下可以存放2年。

所需设备和材料:

- 10 μl、100-200 μl以及多通道移液器
- 带有450 nm滤光片的酶标仪
- 96孔培养板
- CO_2培养箱

概述

Cell Counting Kit-8 (CCK-8) 利用了Dojindo开发的水溶性四唑盐 — WST®-8 (2-(2-甲氧基-4-硝苯基)-3-(4-硝苯基)-5-(2,4-二磺基苯)-2H-四唑单钠盐)，它在电子载体1-Methoxy PMS存在的情况下能够被还原成水溶性的甲臜染料，如图1所示。

WST®：WST是同仁化学研究所的注册商标

CCK-8溶液可以直接加入到细胞样品中；不需要预配各种成分。CCK-8法是用于测定细胞增殖或毒性实验中活细胞数目的一种高灵敏度，无放射性的比色检测法。WST®-8被细胞内脱氢酶氧化还原后生成的橙黄色甲臜染料能够溶解在组织培养基中 (如图2所示)，生成的甲臜量与活细胞数量成正比。

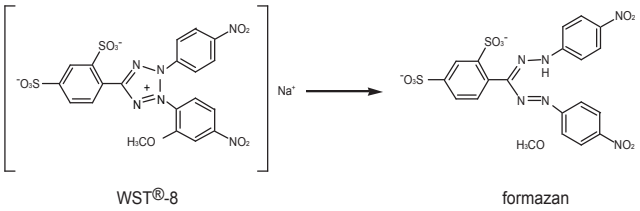

图1. WST®-8和WST®-8甲臜的结构

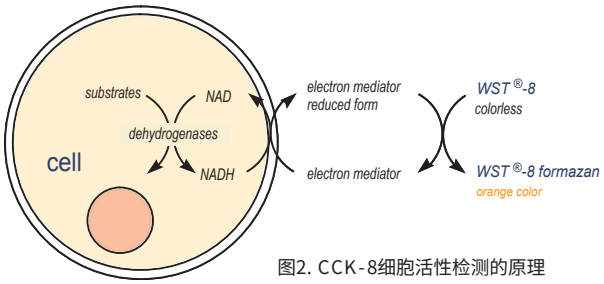

图2. CCK-8细胞活性检测的原理

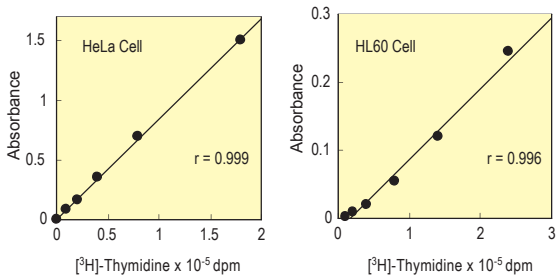

图3. CCK-8法与[3H]-thymidine掺入法之间的相关性

Medium: HeLa.....MEM, 10% FBS
HL60.....RPMI1640, 10% FBS
[3H]-Thymidine.....37 KBq/well
Reagent: CCK-8.....10 µl/well
[3H]-Thymidine assay.....4hours
Incubation: CCK-8.....3 hours

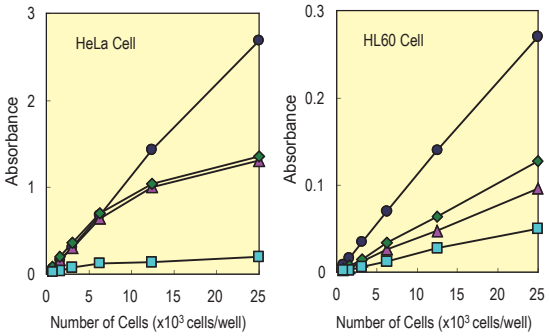

图4. 使用CCK-8与其他试剂灵敏度的比较

Medium : HeLa.....MEM, 10% FBS
HL60.....RPMI1640, 10% FBS
Incubation : HeLa.....37°C, 5 % CO2, 2 hours
HL60.....37°C, 5 % CO2, 3 hours
Detection : CCK-8 (●) ....450 nm, XTT (◆) ....450 nm
MTS (▲) .....490 nm, MTT (■) ...570 nm

操作说明

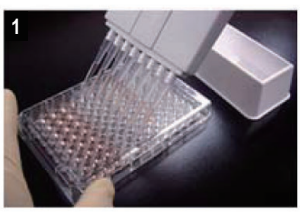

1 在96孔板中每孔加入100 µl的细胞悬液

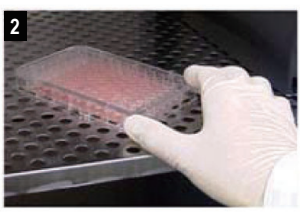

2 在培养箱中预培养细胞

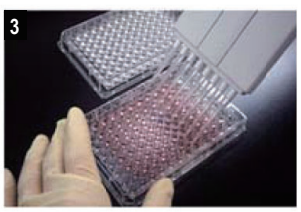

3 向培养板中加入药物 (如果不加药物，可直接进行第5步操作)

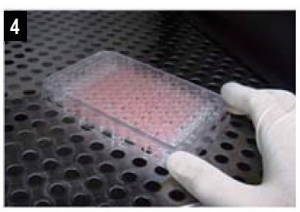

4 在培养箱中培养一段时间

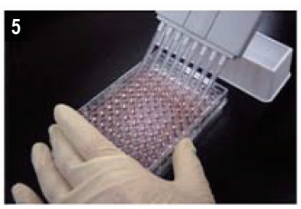

5 向每孔加入10 µl CCK-8溶液

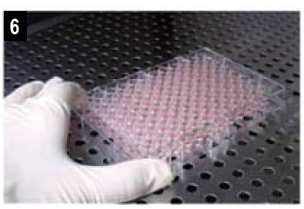

6 在培养箱中培养1-4小时 (可根据自己的实验情况调整时间)

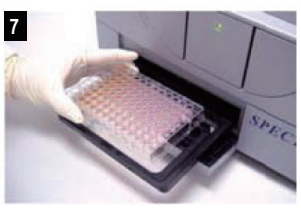

7 用酶标仪测定在450 nm处的吸光度

制作标准曲线

1. 先用细胞计数板计数所制备的细胞悬液中的细胞数量，然后接种细胞。
2. 按比例 (例如：1/2比例) 依次用培养基等比稀释成一个细胞浓度梯度，一般要做3-5个细胞浓度梯度，每组3-6个复孔。
3. 接种后培养2-4小时使细胞贴壁，然后加CCK-8试剂培养一定时间后测定O.D值，制作出一条以细胞数量为横坐标 (X轴)，O.D值为纵坐标 (Y轴) 的标准曲线。根据此标准曲线可以测定出未知样品的细胞数量 (使用此标准曲线的前提条件是实验的条件要一致，便于确定细胞的接种数量以及加入CCK-8后的培养时间)。

*如果暂时不测定O.D值，打算以后测定或为了避免每次准备标准曲线，可以向每孔中加入10 μl Stop Solution，并遮盖培养板避光保存在0-5°C条件下。在7天内吸光度不会发生变化。

细胞增殖—毒性检测

1. 在96孔板中配制100 μl的细胞悬液。**将培养板在培养箱预培养24小时** (在37°C，5% CO_2的条件下)。
2. 向培养板加入10 μl不同浓度的待测物质。
3. **将培养板在培养箱培养一段适当的时间 (例如: 6, 12, 24或48小时)。**
4. 向每孔加入10 μl CCK-8溶液 (**注意不要在孔中生成气泡，它们**会影响O.D值的读数)。
5. 将培养板在培养箱内培养1-4小时。
6. 用酶标仪测定在450 nm处的吸光度。

*如果暂时不测定O.D值，打算以后测定，可以向每孔中加入10 μl Stop Solution，并遮盖培养板避光保存在0-5°C条件下，在7天内吸光度不会发生变化。

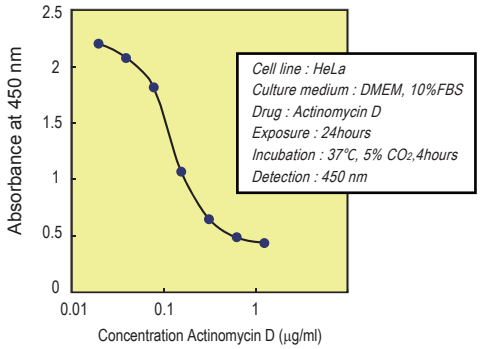

图5. 细胞毒性试验 (Actinomycin D)

计算公式：

细胞存活率 = [(As-Ab) / (Ac-Ab)]×100%

抑制率 = [(Ac-As) / (Ac-Ab)]×100%

As：实验孔(含有细胞的培养基、CCK-8、待测物质)

Ac：对照孔(含有细胞的培养基、CCK-8、没有待测物质)

Ab：空白孔(不含细胞和待测物质的培养基、CCK-8)

细胞活性检测

1. 在96孔板中接种细胞悬液 (100 μl /孔)。将培养板放在培养箱预培养 (在37°C，5% CO_2的条件下)。
2. 向每孔加入10 μl的CCK- 8溶液 (注意不要在孔中生成气泡，它们会影响O.D值的读数)。
3. 将培养板在培养箱内培养1-4小时。
4. 用酶标仪测定在450 nm处的吸光度。

*如果暂时不测定O.D值，打算以后测定，可以向每孔中加入10 μl Stop Solution，并遮盖培养板避光保存在0-5°C条件下，在7天内吸光度不会发生变化。

注意：如果待测物质有氧化性或还原性，可在加CCK-8之前更换新鲜培养基，去掉待测物质的影响。当然待测物质影响比较小的情况可以不更换培养基，直接扣除培养基中加入待测物质后的空白吸收即可。

关联产品

应用	产品名称	货号	规格
细胞活性检测-化学发光法	Cell Counting Kit-Luminescence	CK18	200T
细胞毒性检测	Cytotoxicity LDH Assay Kit-WST	CK12	500T
活死细胞双染	Calcein-AM/PI Double Staining Kit	C542	500T
细胞凋亡检测	Annexin V, FITC Apoptosis Detection Kit	AD10	50T
	Annexin V, 633 Apoptosis Detection Kit	AD11	50T
	Caspase-3 Assay Kit -Colorimetric-	C551	50T
细胞周期检测	Cell Cycle Assay Kit - PI/RNase Staining	C543	50T
ROS检测	ROS Assay Kit -Highly Sensitive DCFH- DA	R252	100T
线粒体自噬检测	Mitophagy Detection Kit	MD01	1 set
线粒体染色	MitoBright LT Green, Red, Deep Red	MT10,11,12	20 μl, 400 μl
线粒体膜电位检测	JC-1 MitoMP Detection Kit	MT09	1 set
线粒体超氧化物检测	MT-1 MitoMP Detection Kit	MT13	1 set
	mtSOX Deep Red -Mitochondrial Superoxide Detection	MT14	1 set, 3 sets
免疫荧光用线粒体荧光染料	MitoBright IM Red for Immunostaining	MT15	20 μl
脂质过氧化物检测	Liperfluo	L248	50 μg, 50 μg×5
	MitoPeDPP	M466	5 μg×3
细胞二价铁离子(Fe^{2+})检测	FerroOrange	F374	1 tube, 3 tubes
	Mito-FerroGreen	M489	50 μg×2
组织内总铁含量检测	Iron Assay Kit -Colorimetric-	I291	50T
氧化型/还原型谷胱甘肽检测	GSSG/GSH Quantification Kit II	G263	100T

Q&A:

1. 每孔应该接种多少细胞？

贴壁细胞每孔至少需要接种1,000个细胞 (100 μl的培养基)，检测白细胞时由于它的灵敏度较低，每孔至少需要接种2,500个细胞 (100 μl的培养基)，建议先做几个孔摸索接种细胞的数量。如果要使用24孔板或是6孔板实验，请先计算每孔相应的接种量，并按照每孔培养基总体积的10%加入CCK- 8溶液。

2. 如何设定空白对照？

在不含细胞的培养基中加入CCK- 8，测定450 nm的吸光度即为空白对照。在做加药实验 (细胞毒性实验) 时，还应考虑药物的吸收，可在不含细胞，加入药物的培养基中加入CCK- 8，测定450 nm的吸光度作为空白对照。

3. 哪些物质会影响CCK- 8的测定？

当有还原性物质存在时会影响CCK- 8的测定，增加O.D值；在有氧化性物质存在时会抑制测定反应的发生，减小O.D值；在有酚红存在的情况下，会增加空白吸收，但不影响测定，扣除空白吸收即可。

4. 在做加药实验时，药物对测定是否有影响？如何解决？

有时会有影响。如果药物具有还原性，就会和CCK- 8试剂发生显色反应，增加吸光度。解决办法：首先要确认药物是否有吸收，在含有药物的培养基中加入CCK- 8，测定450 nm的吸光度，如果它的吸光度比不含药物的培养基 (只加CCK-8) 的吸光度高，则证明药物有影响，可在加CCK- 8之前更换培养基，去掉药物的影响。

5. CCK- 8对细胞的毒性大小如何？

CCK- 8对细胞的毒性相当低，同样的细胞在CCK- 8法检测后还可用于其他细胞增殖的检测实验，如结晶紫检测法，中性红检测法或DNA荧光检测法等。

6. CCK- 8的保质期有多久？

CCK- 8在避光0-5℃的条件下可以存放2年。在常温下可以保存3周左右，颜色应该为浅红色，
如果颜色发生改变，则可能会增加空白吸光度。

7. 我没有450 nm的滤光片，还可以使用哪些其他的滤光片？

您可以使用吸光度在430-490 nm之间的滤光片，但是450 nm滤光片的检测灵敏度最高。

8. CCK- 8能否对活细胞进行染色?

不能。因为CCK- 8的主要成分是一种水溶性的四唑盐 (WST®- 8)，并通过电子载体1- Methoxy PMS将活细胞中的电子交换到培养基中的WST®- 8上，因为WST®- 8及其生成的甲臜染料是高度水溶性的，不会进入细胞内，所以CCK- 8不能对活细胞进行染色。

9. 必须设定参比波长吗？设定的目的是什么？

不一定要设定，CCK- 8试剂在参比波长处没有吸光度。设定参比波长的目的是为了去除由于样品浑浊所带来的吸收。

10. 如果O.D值太低，可以采取什么办法？

可以采取2个办法：

① 适当增加细胞数量。

② 延长加入CCK- 8试剂后的染色时间。

CCK-8之Science篇:

1. X-ray screening identifies active site and allosteric inhibitors of SARS-CoV-2 main protease, *Science*, **2021**, *372*, 642-646
2. Structure-based design of antiviral drug candidates targeting the SARS-CoV-2 main protease, *Science*, **2020**, *368*, 1331-1335
3. De novo design of potent and resilient hACE2 decoys to neutralize SARS-CoV-2, *Science*, **2020**, *370*, 1208-1214

CCK-8之Nature篇（含子刊）：

1. Chemical modification of PS-ASO therapeutics reduces cellular protein-binding and improves the therapeutic index, *Nature Biotechnology*, **2019**, 37640-650
2. Multi-omic measurements of heterogeneity in HeLa cells across laboratories, *Nature Biotechnology*, **2019**, *37*, 314-322
3. A perfusable, multifunctional epicardial device improves cardiac function and tissue repair, *Nature Medicine*, **2021**, *27*, 480-490
4. Dual effects of carbon monoxide on pericytes and neurogenesis in traumatic brain injury, *Nature Medicine*, **2016**, *22*, 1335-1341
5. Human induced pluripotent stem cell-derived cardiomyocytes recapitulate the predilection of breast cancer patients to doxorubicin-induced cardiotoxicity, *Nature Medicine*, **2016**, *22*(5), 547-556
6. Orphan nuclear receptor NR4A1 regulates transforming growth factor-β signaling and fibrosis, *Nature Medicine*, **2015**, *21*(2), 150-158
7. Randomized dose-finding clinical trial of oncolytic immunotherapeutic vaccinia JX-594 in liver cancer, *Nature Medicine*, **2013**, *19*, 329-336
8. Compromised CDK1 activity sensitizes BRCA-proficient cancers to PARP inhibition, *Nature Medicine*, **2011**, *17*(7), 875-882
9. Mesenchymal stem cell-based tissue regeneration is governed by recipient T lymphocytes via IFN-γ and TNF-α, *Nature Medicine*, **2011**,*17*(12), 1594-1601
10. Monoclonal antibody targeting of N-cadherin inhibits prostate cancer growth, metastasis and castration resistance, *Nature Medicine*, **2010**, *16*(12), 1414-1420
11. Identification of tendon stem/progenitor cells and the role of the extracellular matrix in their niche, *Nature Medicine*, **2007**, *13*(10), 1219-1227
12. Altered TMPRSS2 usage by SARS-CoV-2 Omicron impacts infectivity and fusogenicity, *Nature*, **2022**, doi.org/10.1038/s41586-022-04474-x
13. DAXX represents a new type of protein-folding enabler, *Nature*, **2021**, *597,*132-137
14. DHODH-mediated ferroptosis defence is a targetable vulnerability in cancer, *Nature*, **2021**, *593*, 586-590
15. Dietary fructose improves intestinal cell survival and nutrient absorption, *Nature*, **2021**, *597*, 263-267
16. Epigenetic therapy inhibits metastases by disrupting premetastatic niches, *Nature*, **2020**, doi.org/10.1038/s41586-020-2054-x
17. ILC2s amplify PD-1 blockade by activating tissue-specific cancer immunity, *Nature*, **2020**, *579*, 130-135
18. Potential circadian effects on translational failure for neuroprotection, *Nature*, **2020**, *582*, 395-398
19. Chimeric peptidomimetic antibiotics against Gram-negative bacteria, *Nature*, **2019**, doi:10.1038/s41586-019-1665-6
20. PU.1 controls fibroblast polarization and tissue fibrosis, *Nature*, **2019**, *566*, 344-349
21. Mitochondrial unfolded protein response controls matrix pre-RNA processing and translation, *Nature*, **2016**, *534*, 710-713
22. Transfer of mitochondria from astrocytes to neurons after stroke, *Nature*, **2016**, *535*, 551-555
23. Signalling thresholds and negative B-cell selection in acute lymphoblastic leukaemia, *Nature*, **2015**, *521*, 357–361
24. The sonic hedgehog factor GLI1 imparts drug resistance through inducible glucuronidation, *Nature*, **2014**, *511*(7507), 90-93
25. Sema3A regulates bone-mass accrual through sensory innervations, *Nature*, **2013**, *497*(7450), 490-493
26. Acetylation-dependent regulation of endothelial Notch signalling by the SIRT1 deacetylase, *Nature*, **2011**, *473*(7346), 234-238
27. Embryonic lethal phenotype reveals a function of TDG in maintaining epigenetic stability, *Nature*, **2011**, *470*(7334), 419-423
28. Intravenous delivery of a multi-mechanistic cancer-targeted oncolytic poxvirus in humans, *Nature*, **2011**, *477*(7362), 99-102
29. Frequent inactivation of A20 in B-cell lymphomas, *Nature*, **2009**, *459*(7247), 712-716
30. Modulation of microRNA processing by p53, *Nature*, **2009**, *460*(7254), 529-533
31. Oncogenic mutations of ALK kinase in neuroblastoma, *Nature*, **2008,** *455*(7215), 971-974
32. Hyaluronic acid-bilirubin nanomedicine for targeted modulation of dysregulated intestinal barrier, microbiome and immune responses in colitis, *Nature Materials*, **2019**, doi: 10.1038/s41563-019-0462-9
33. Parenchymal and stromal tissue regeneration of tooth organ by pivotal signals reinstated in decellularized matrix, *Nature Materials*, **2019**, *18*(6), 627-637
34. Guiding intracortical brain tumour cells to an extracortical cytotoxic hydrogel using aligned polymeric nanofibres, *Nature Materials*, **2014**, *13*(3), 308-316
35. Precise targeting of POLR2A as a therapeutic strategy for human triple negative breast cancer, *Nature Nanotechnology*, **2019**, *14*, 388-397
36. Metal nanoparticles in the presence of lipopolysaccharides trigger the onset of metal allergy in mice, *Nature Nanotechnology*, **2016**, *11*, 808-816

CCK-8之Nature篇（含子刊）：

37. Cross-species chromatin interactions drive transcriptional rewiring in Epstein–Barr virus–positive gastric adenocarcinoma, *Nature Genetics*, **2020**, doi: 10.1038/s41588-020-0665-7
38. Transposable elements drive widespread expression of oncogenes in human cancers, *Nature Genetics*, **2019**, *51*, 611-617
39. Exome-wide analyses identify low-frequency variant in CYP26B1 and additional coding variants associated with esophageal squamous cell carcinoma, *Nature Genetics*, **2018**, *50*, 338-343
40. Pancreatic cancer risk variant in LINC00673 creates a miR-1231 binding site and interferes with PTPN11 degradation, *Nature Genetics*, **2016**, *48*, 747-757
41. Whole-genome mutational landscape and characterization of noncoding and structural mutations in liver cancer, *Nature Genetics*, **2016**, *48*, 500-509
42. A recurrent inactivating mutation in RHOA GTPase in angioimmunoblastic T cell lymphoma, *Nature Genetics*, **2014**, *46*, 371-375
43. Exome sequencing identifies somatic gain-of-function PPM1D mutations in brainstem gliomas, *Nature Genetics*, **2014**, *46*, 726-730
44. Somatic RHOA mutation in angioimmunoblastic T cell lymphoma, *Nature Genetics*, **2014**, *46*, 171-175
45. Genome-wide association study identifies common variants in SLC39A6 associated with length of survival in esophageal squamous-cell carcinoma, *Nature Genetics*, **2013**, *45*(6), 632-638
46. Recurrent mutations in multiple components of the cohesin complex in myeloid neoplasms, *Nature Genetics*, **2014**, *45*, 1232-1237
47. Common variants at 11q12, 10q26 and 3p11.2 are associated with prostate cancer susceptibility in Japanese, *Nature Genetics*, **2012**, *44*(4), 426-429
48. Exome sequencing of hepatitis B virus-associated hepatocellular carcinoma, *Nature Genetics*, **2012**, *44*(10), 1117-1121
49. LIN28B induces neuroblastoma and enhances MYCN levels via let-7 suppression, *Nature Genetics*, **2012**, *44*(11), 1199-1206
50. Heterozygosity with respect to Zfp148 causes complete loss of fetal germ cells during mouse embryogenesis, *Nature Genetics*, **2003**, *33*, 172-176
51. The tumor suppressor PTEN has a critical role in antiviral innate immunity, *Nature Immunology*, **2016**, *17*, 241-249
52. Neddylation of PTEN regulates its nuclear import and promotes tumor development, *Cell Research*, **2021**, *31*, 291-311
53. Pericytes augment glioblastoma cell resistance to temozolomide through CCL5-CCR5 paracrine signaling, *Cell Research*, **2021**, https://doi.org/10.1038/s41422-021-00528-3
54. SIDT1-dependent absorption in the stomach mediates host uptake of dietary and orally administered microRNAs, *Cell Research*, **2021**, *31*, 247-258
55. Inhibition of SARS-CoV-2 (previously 2019-nCoV) infection by a highly potent pan-coronavirus fusion inhibitor targeting its spike protein that harbors a high capacity to mediate membrane fusion, *Cell Research*, **2020**, *30*, 343-355
56. The role of ferroptosis in ionizing radiation-induced cell death and tumor suppression, *Cell Research*, **2020**, *30*, 146-162
57. A two-step lineage reprogramming strategy to generate functionally competent human hepatocytes from fibroblasts, *Cell Research*, **2019**, *29*, 696-710
58. Expansion and differentiation of human hepatocyte-derived liver progenitor-like cells and their use for the study of hepatotropic pathogens, *Cell Research*, **2019**, *29*, 8-22
59. PARylation regulates stress granule dynamics, phase separation, and neurotoxicity of disease-related RNA-binding proteins, *Cell Research*, **2019**, *29*, 233-247
60. A dynamic N6-methyladenosine methylome regulates intrinsic and acquired resistance to tyrosine kinase inhibitors, *Cell Research*, **2018**, *28*, 1062-1076
61. An NF90/NF110-mediated feedback amplification loop regulates dicer expression and controls ovarian carcinoma progression, *Cell Research*, **2018**, *28*, 556-571
62. Integrated genomic analysis identifies deregulated JAK/STAT-MYC-biosynthesis axis in aggressive NK-cell leukemia, *Cell Research*, **2018**, *28*, 172-186
63. Existing drugs as broad-spectrum and potent inhibitors for Zika virus by targeting NS2B-NS3 interaction, *Cell Research*, **2017**, *27*, 1046-1064
64. Epigenetic silencing of microRNA-149 in cancer-associated fibroblasts mediates prostaglandin E2/interleukin-6 signaling in the tumor microenvironment, *Cell Research*, **2015**, *25*, 588-603

CCK-8之Cell篇（含子刊）:

1. Virological characteristics of the SARS-CoV-2 Omicron BA.2 spike, *Cell*, **2022**, doi.org/10.1016/j.cell.2022.04.035
2. In Vivo CRISPR Screens Identify E3 Ligase Cop1 as a Modulator of Macrophage Infiltration and Cancer Immunotherapy Target, *Cell*, **2021**, DOI:https://doi.org/10.1016/j.cell.2021.09.006
3. A Bacterial Effector Reveals the V-ATPase-ATG16L1 Axis that Initiates Xenophagy, *Cell*, **2019**, *178*(3), 552-566
4. Higher-Order Clustering of the Transmembrane Anchor of DR5 Drives Signaling, *Cell*, **2019**, *176*(6), 1477-1489
5. Insulin Receptor Associates with Promoters Genome-wide and Regulates Gene Expression, *Cell*, **2019**, *177*(3), 722-736
6. B-Cell-Specific Diversion of Glucose Carbon Utilization Reveals a Unique Vulnerability in B Cell Malignancies, *Cell*, **2018**, *173*(2), 470-484
7. Fusobacterium nucleatum Promotes Chemoresistance to Colorectal Cancer by Modulating Autophagy, *Cell*, **2017**,*170*(3), 548-563
8. Methyltransferase SETD2-Mediated Methylation of STAT1 Is Critical for Interferon Antiviral Activity, *Cell*, **2017**, *170*(3), 492-506
9. Loss of 5-Hydroxymethylcytosine Is an Epigenetic Hallmark of Melanoma, *Cell*, **2012**, *150*(6), 1135-1146
10. Mapping the Hallmarks of Lung Adenocarcinoma with Massively Parallel Sequencing, *Cell*, **2012**, *150*(6), 1107-1120
11. Iron-Export Ferroxidase Activity of β-Amyloid Precursor Protein Is Inhibited by Zinc in Alzheimer's Disease, *Cell*, **2010**, *142*(6), 857-867
12. Autocrine VEGF Signaling Is Required for Vascular Homeostasis, *Cell*, **2007**, *130*(4), 691-703
13. Genomic and Transcriptomic Characterization of Natural Killer T Cell Lymphoma, *Cancer Cell*, **2020**, *37*, 403-419
14. CDK7 Inhibition Potentiates Genome Instability Triggering Anti-tumor Immunity in Small Cell Lung Cancer, *Cancer Cell*, **2020**, *37*, 37-54
15. Wild-Type p53 Promotes Cancer Metabolic Switch by Inducing PUMA-Dependent Suppression of Oxidative Phosphorylation, *Cancer Cell*, **2019**, *35*(2), 191-203
16. Genomic and Epigenomic Profiling of High-Risk Intestinal Metaplasia Reveals Molecular Determinants of Progression to Gastric Cancer, *Cancer Cell*, **2018**, *33*(1), 137-150
17. Transcriptional Regulation of the Warburg Effect in Cancer by SIX1, *Cancer Cell*, **2018**, *33*(3), 368-385
18. Enhanced Fructose Utilization Mediated by SLC2A5 Is a Unique Metabolic Feature of Acute Myeloid Leukemia with Therapeutic Potential, *Cancer Cell*, **2016**, *30*(5), 779-791
19. Targeting Transcriptional Addictions In Small Cell Lung Cancer With a Covalent CDK7 Inhibitor, *Cancer Cell*, **2014**, *26*(6), 909-922
20. Nrf2 Redirects Glucose and Glutamine into Anabolic Pathways in Metabolic Reprogramming, *Cancer Cell*, **2012**, *22*(1), 66-79
21. Polycomb-Mediated Loss of miR-31 Activates NIK-Dependent NF-kB Pathway in Adult T Cell Leukemia and Other Cancers, *Cancer Cell*, **2012**, *21*(1), 121-135
22. E2F1-Regulated MicroRNAs Impair TGFβ-Dependent Cell-Cycle Arrest and Apoptosis in Gastric Cancer, *Cancer Cell*, **2008**, *13*, 272-286
23. An Upstream Open Reading Frame in Phosphatase and Tensin Homolog Encodes a Circuit Breaker of Lactate Metabolism, *Cell Metabolism*, **2021**, *33*, 28-144
24. Apaf-1 Pyroptosome Senses Mitochondrial Permeability Transition, *Cell Metabolism*, **2021**, *33*, 1-13
25. Metabolic-Pathway-Based Subtyping of Triple[1]Negative Breast Cancer Reveals Potential Therapeutic Targets, *Cell Metabolism*, **2021**, *33*, 1-14
26. A Novel Allosteric Inhibitor of Phosphoglycerate Mutase 1 Suppresses Growth and Metastasis of Non-Small-Cell Lung Cancer, *Cell Metabolism*, **2019**, *30*(6), 1107-1119
27. IGF-2 Preprograms Maturing Macrophages to Acquire Oxidative Phosphorylation-Dependent Anti-inflammatory Properties, *Cell Metabolism*, **2019**, *29*(6), 1363-1375
28. Liver damage, inflammation, and enhanced tumorigenesis after persistent mTORC1 inhibition, *Cell Metabolism*, **2014**, *20*(1), 133-44
29. Loss of SATB1 Induces p21-Dependent Cellular Senescence in Post-mitotic Dopaminergic Neurons, *Cell Stem Cell*, **2019**, *25*(4), 514-530
30. PPM1D Mutations Drive Clonal Hematopoiesis in Response to Cytotoxic Chemotherapy, *Cell Stem Cell*, **2018,** *23*(5), 700-713
31. Lipid Desaturation Is a Metabolic Marker and Therapeutic Target of Ovarian Cancer Stem Cells, *Cell Stem Cell*, **2017**, *20*(3), 303-314

CCK-8之高分篇:

1. The effect of novel acridine-based agents with topoisomerase II inhibitor on mesothelioma cell proliferation and apoptosis, *Journal of Clinical Oncology*, **2011**, *15*, DOI:10.1200/jco.2011.29.15_suppl.e13507
2. Genetic risk of extranodal natural killer T-cell lymphoma: a genome-wide association study in multiple populations, *Lancet Oncology*, **2019**, pii: S1470-2045(19)30799-5
3. A Secondary Mutation in BRAF Confers Resistance to RAF Inhibition in a BRAF V600E-Mutant Brain Tumor, *Cancer Discovery*, **2018**, *8*(9),1130-1141
4. Epigenomic Promoter Alterations Amplify Gene Isoform and Immunogenic Diversity in Gastric Adenocarcinoma, *Cancer Discovery*, **2017**, *7*(6), 630-651
5. A novel photothermally controlled multifunctional scaffold for clinical treatment of osteosarcoma and tissue regeneration, *Materials Today*, **2020**, doi.org/10.1016/j.mattod.2019.12.005
6. 3D Heterogeneous Device Arrays for Multiplexed Sensing Platforms Using Transfer of Perovskites, *Advanced Materials*, **2021**, *33*, 2101093
7. Hydroxyapatite Nanorods Function as Safe and Effective Growth Factors Regulating Neural Differentiation and Neuron Development, *Advanced Materials*, **2021**, 2100895
8. Self-Activatable Photo-Extracellular Vesicle for Synergistic Trimodal Anticancer Therapy, *Advanced Materials*, **2021**, *33*, 2005562
9. Stretchable and Highly Permeable Nanofibrous Sensors for Detecting Complex Human Body Motion, *Advanced Materials*, **2021**, 2102488
10. A Graphdiyne Oxide-Based Iron Sponge with Photothermally Enhanced Tumor-Specific Fenton Chemistry, *Advanced Materials*, **2020**, 2000038
11. A Highly Efficient Tumor-Targeting Nanoprobe with a Novel Cell Membrane Permeability Mechanism, *Advanced Materials*, **2019**, *31*(12), e1807456
12. A Self-Pumping Dressing for Draining Excessive Biofluid around Wounds, *Advanced Materials*, **2019**, *31*(5), e1804187
13. Biomimetic Metal-Organic Framework Nanoparticles for Cooperative Combination of Antiangiogenesis and Photodynamic Therapy for Enhanced Efficacy, *Advanced Materials*, **2019**, *31*(15), 1808200
14. CD44-Specific A6 Short Peptide Boosts Targetability and Anticancer Efficacy of Polymersomal Epirubicin to Orthotopic Human Multiple Myeloma, *Advanced Materials*, **2019**, doi.org/10.1002/adma.201904742
15. Chirality Controls Mesenchymal Stem Cell Lineage Diversification through Mechanoresponses, *Advanced Materials*, **2019**, doi.org/10.1002/adma.201900582
16. Engineering Biomimetic Platesomes for pH-Responsive Drug Delivery and Enhanced Antitumor Activity, *Advanced Materials*, **2019**, *31*(32), e1900795
17. Highly Efficient and Environmentally Friendly Fabrication of Robust, Programmable, and Biocompatible Anisotropic, All-Cellulose, Wrinkle-Patterned Hydrogels for Cell Alignment, *Advanced Materials*, **2019**, *31*(46), e1904762
18. Securing the Payload, Finding the Cell, and Avoiding the Endosome: Peptide-Targeted, Fusogenic Porous Silicon Nanoparticles for Delivery of siRNA, *Advanced Materials*, **2019**, *31*(35), e1902952
19. Semiconducting Polymer Nanoparticles for Centimeters-Deep Photoacoustic Imaging in the Second Near-Infrared Window, *Advanced Materials*, **2017**, *29*(41), 1703403
20. Structurally and Functionally Optimized Silk-Fibroin-Gelatin Scaffold Using 3D Printing to Repair Cartilage Injury In Vitro and In Vivo, *Advanced Materials*, **2017**, *29*(29), doi: 10.1002/adma.201701089
21. DNA-Nanostructure-Gold-Nanorod Hybrids for Enhanced In Vivo Optoacoustic Imaging and Photothermal Therapy, *Advanced Materials*, **2016**, *28*(45):10000-10007

网址：http://www.dojindo.cn E-mail: info@dojindo.cn

如果您需要更多的信息或者有任何问题可以通过以下的方式联系我们:

东仁化学科技 (上海) 有限公司
上海
上海市零陵路899号飞洲国际广场27楼J座
邮编：200030
电话：400-823-9388

北仁化学科技 (北京) 有限公司
北京
北京市朝阳区德外马甸裕民路12号元辰鑫大厦E1-210室
邮编：100029
电话：010-8225-1765

2022年6月印刷